

A quasi-pure Bose-Einstein condensate immersed in a Fermi sea

F. Schreck, L. Khaykovich, K. L. Corwin, G. Ferrari*, T. Bourdel, J. Cubizolles, and C. Salomon
Laboratoire Kastler Brossel, Ecole Normale Supérieure, 24 rue Lhomond, 75231 Paris CEDEX 05, France
 * :LENS-INFN, Largo E. Fermi 2, Firenze 50125 Italy.

(October 22, 2018)

We report the observation of co-existing Bose-Einstein condensate and Fermi gas in a magnetic trap. With a very small fraction of thermal atoms, the ${}^7\text{Li}$ condensate is quasi-pure and in thermal contact with a ${}^6\text{Li}$ Fermi gas. The lowest common temperature is $0.28\ \mu\text{K} \simeq 0.2(1) T_C = 0.2(1) T_F$ where T_C is the BEC critical temperature and T_F the Fermi temperature. Behaving as an ideal gas in the radial trap dimension, the condensate is one-dimensional.

PACS numbers: 05.30.Fk, 05.30.Jp, 03.75.-b, 05.20.Dd, 32.80.Pj

Bose-Einstein condensation of atomic gases has been very actively studied in recent years [1,2]. Because of the dilute character of the samples and the ability to control the atom-atom interactions, for the first time a detailed comparison with the theories of quantum gases has been made. Fermi gases, on the other hand, have only been investigated experimentally for two years [3–5]. They are predicted to possess intriguing properties and may offer an interesting link with the behavior of electrons in metals and semiconductors, and the possibility of Cooper pairing [6] such as in high temperature superconductors and neutron stars. Mixtures of bosonic and fermionic quantum systems, with the prominent example of ${}^4\text{He}$ - ${}^3\text{He}$ fluids, have also stimulated intense theoretical and experimental activity [7]. This has led to new physical effects including phase separation, influence of the superfluidity of the Bose system on the Fermi degeneracy and to new applications such as the dilution refrigerator [7–9].

In this paper, we present a new mixture of bosonic and fermionic systems, a stable Bose-condensed gas immersed in a Fermi sea. Confined in the same magnetic trap, both atomic species are in thermal equilibrium with a temperature of $0.2(1) T_F \ll T_C$. The condensate is made of ${}^7\text{Li}$ atoms in internal state $|F = 1, m_F = -1\rangle$ while the degenerate Fermi gas is made of ${}^6\text{Li}$ atoms in $|F = 1/2, m_F = -1/2\rangle$ (fig. 1). All previous experiments performed with ${}^7\text{Li}$ in $|F = 2, m_F = 2\rangle$ had condensate numbers limited to $N \leq 1400$ because of the negative scattering length, $a = -1.4\ \text{nm}$, in this state [10,11]. Our condensate is produced in a state which has a positive, but small, scattering length, $a = +0.27\ \text{nm}$ [12]. The number of condensate atoms is typically 10^4 , and BEC appears unambiguously both in the position distribution in the trap and in the standard time of flight images. An interesting feature is the one-dimensional character of this condensate, behaving as an ideal gas in the transverse direction of the trap [13,14].

Because of the symmetrization postulate, colliding fermions have no s -wave scattering at low energy and the p -wave contribution vanishes in the low temperature domain of interest. Our method for producing simultaneous quantum degeneracy for both isotopes

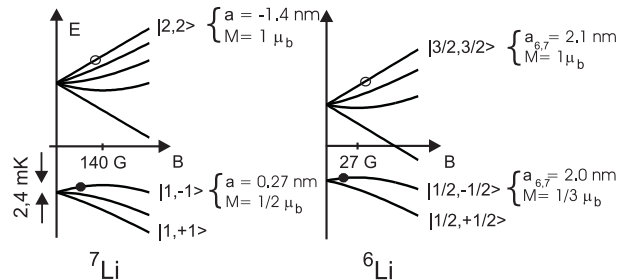


FIG. 1. Energy levels of ${}^7\text{Li}$ and ${}^6\text{Li}$ ground states in a magnetic field. Relevant scattering lengths, a , and magnetic moments, M , are given. μ_b is the Bohr magneton. The $|1, -1\rangle$ state (resp. $|1/2, -1/2\rangle$) is only trapped in fields weaker than 140 Gauss (resp. 27 Gauss). Open circles: first cooling stage; black circles: second cooling stage.

of lithium is sympathetic cooling [4,5]; s -wave collisions between two different atomic isotopes are allowed and RF evaporation selectively removes from the trap high energy atoms of one species. Elastic collisions subsequently restore thermal equilibrium of the two-component gas at a lower temperature. Our experimental setup has been described in detail in [4,15]. A mixture of ${}^6\text{Li}$ and ${}^7\text{Li}$ atoms is loaded from a magneto-optical trap into a strongly confining Ioffe-Pritchard trap at a temperature of about 2 mK. As depicted in fig.1, this relatively high temperature precludes direct magnetic trapping of the atoms in their lower hyperfine state because of the shallow magnetic trap depth, 2.4 mK for ${}^7\text{Li}$ in $|F = 1, m_F = -1\rangle$ and 0.2 mK for ${}^6\text{Li}$ in $|F = 1/2, m_F = -1/2\rangle$. Therefore we proceed in two steps. Both isotopes are first trapped and cooled in their upper hyperfine states. There is no limitation for the trap depth and the confinement is better because the magnetic moment is higher. Evaporation is performed selectively on ${}^7\text{Li}$ using a microwave field near 803 MHz that couples $|F = 2, m_F = 2\rangle$ to $|F = 1, m_F = 1\rangle$. When both gases are cooled to a common temperature of about $9\ \mu\text{K}$, atoms are transferred using a combination of microwave and RF pulses into states $|F = 1, m_F = -1\rangle$ and $|F = 1/2, m_F = -1/2\rangle$ with an energy far below their respective trap depths. Evaporative cooling is then resumed until the BEC threshold is reached for

${}^7\text{Li}$.

In the first series of experiments, both Li isotopes are trapped in their higher HF states. ${}^6\text{Li}$ is sympathetically cooled to Fermi degeneracy by performing 30 seconds of evaporative cooling on ${}^7\text{Li}$ [4]. Trap frequencies for ${}^7\text{Li}$ are $\omega_{\text{rad}} = 2\pi * 4000(10)s^{-1}$ and $\omega_{\text{ax}} = 2\pi * 75.0(1)s^{-1}$ with a bias field of 2 G. Absorption images of both isotopes are recorded on a single CCD camera with a resolution of $10\ \mu\text{m}$. Images are taken quasi-simultaneously (only 1 ms apart) in the trap or after a time of flight expansion. Probe beams have an intensity below saturation and a common duration of $30\ \mu\text{s}$. Typical in-situ absorption images in the quantum regime can be seen in fig.2. Here the temperature T is $1.4(1)\ \mu\text{K}$ and $T/T_F = 0.33(5)$, where the Fermi temperature T_F is $(\hbar\bar{\omega}/k_B)(6N_F)^{1/3}$, with $\bar{\omega}$ the geometric mean of the three oscillation frequencies in the trap and N_F the number of fermions. For images recorded in the magnetic trap, the common temperature is measured from the spatial extent of the bosonic cloud in the axial direction since the shape of the Fermi cloud is much less sensitive to temperature changes when $T/T_F < 1$ [18]. The spatial distributions of bosons and fermions are recorded after a 1 sec thermalization stage at the end of the evaporation. As the measured thermalization time constant between the two gases, 0.15 s, is much shorter than 1 s, the two clouds are in thermal equilibrium. Both isotopes experience the same trapping potential. Thus the striking difference between the sizes of the Fermi and Bose gases [5] is a direct consequence of Fermi pressure. The measured axial profiles in fig.2 are in excellent agreement with the calculated ones (solid lines) for a Bose distribution at the critical temperature T_C . In our steepest traps, Fermi temperatures as high as $11\ \mu\text{K}$ with a degeneracy of $T/T_F = 0.36$ are obtained. This T_F is a factor 3 larger than the single photon recoil temperature at 671 nm, opening interesting possibilities for light scattering experiments [22].

Our highest Fermi degeneracy in the ${}^6\text{Li}$ $F = 3/2$ state is $T/T_F = 0.25(5)$ with $T_F = 4\ \mu\text{K}$, very similar to ref. [5]. This limit is set by the fact that the boson temperature cannot be lowered below T_C . Because of the negative scattering length in ${}^7\text{Li}$, $|F = 2, m = 2\rangle$, the number of condensed atoms cannot exceed ~ 300 in our trap [10]. This, together with the condition that sympathetic cooling stops when the heat capacity of the bosons approximately equals that of the fermions, limits the Fermi degeneracy to about 0.3 [5].

In order to explore the behavior of a Fermi sea in the presence of a BEC with a temperature well below T_C , we perform another series of experiments with both isotopes trapped in their lower HF state. As the ${}^7\text{Li}$ scattering length is then positive (fig.1), a stable BEC with high atom numbers is now possible. To avoid large dipolar relaxation, ${}^6\text{Li}$ must also be in its lower HF state [17]. First, sympathetic cooling is performed on the initial stretched states to $\sim 9\ \mu\text{K}$.

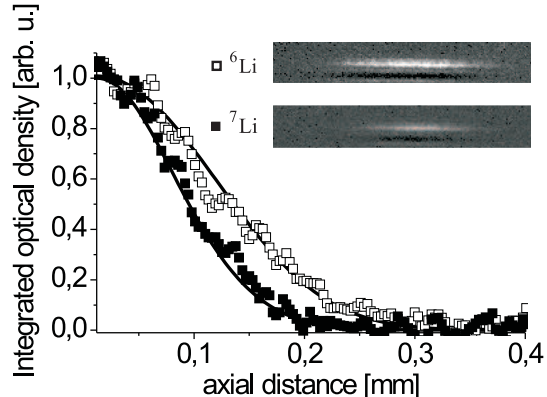


FIG. 2. Observation of Fermi pressure. Absorption images in the trap and spatial distributions integrated over the vertical direction of $8.1 \cdot 10^4$ ${}^6\text{Li}$ and $2.7 \cdot 10^4$ ${}^7\text{Li}$ atoms in their higher hyperfine states. The temperature is $1.4(1)\ \mu\text{K}$ corresponding to T_C for the bosons and $0.33(5)T_F$ for the fermions. Solid lines are the expected Bose and Fermi distributions.

Then, to facilitate state transfer, the trap is adiabatically opened to frequencies $\omega_{\text{rad}} = 2\pi * 100\ s^{-1}$ and $\omega_{\text{ax}} = 2\pi * 5\ s^{-1}$ (for ${}^7\text{Li}$, $F=2$). The transfer of each isotope uses two microwave π pulses. The first pulse at 803 MHz for ${}^7\text{Li}$ (228 MHz for ${}^6\text{Li}$) transfers the atoms from $|2, 2\rangle$ to $|1, 1\rangle$ ($|3/2, 3/2\rangle$ to $|1/2, 1/2\rangle$), a magnetically untrapped state (see fig.1). The second RF π pulse at 1 MHz (1.3 MHz) transfers them to $|1, -1\rangle$ ($|1/2, -1/2\rangle$) a magnetically trapped state. Adiabatic opening of the trap cools the cloud, therefore decreasing the energy broadening of the resonance and giving more time for the passage through untrapped states. The duration of the π pulses are $17\ \mu\text{s}$ and $13\ \mu\text{s}$ and more than 70% of each isotope are transferred. Finally the trap is adiabatically recompressed to the steepest confinement giving $\omega_{\text{rad}} = 2\pi * 4970(10)s^{-1}$ and $\omega_{\text{ax}} = 2\pi * 83(1)s^{-1}$ for ${}^7\text{Li}$ $|F = 1, m = -1\rangle$, compensating for the reduced magnetic moment.

Because of the very large reduction of the ${}^7\text{Li}$ s -wave scattering cross section (by a factor of 28) from the $F=2$ to the $F=1$ state, we were unable to reach runaway evaporation with ${}^7\text{Li}$ atoms alone in $F = 1$. In contrast, the ${}^6\text{Li}/{}^7\text{Li}$ cross section is 28 times higher than the ${}^7\text{Li}/{}^7\text{Li}$ one. We therefore use ${}^6\text{Li}$ atoms as a buffer gas to accelerate the thermalization rate of both gases. Two different methods were used to perform the evaporation. The first consists in using two RF ramps on the HF transitions of ${}^6\text{Li}$ (from $|1/2, -1/2\rangle$ to $|3/2, -3/2\rangle$) and ${}^7\text{Li}$ (from $|1, -1\rangle$ to $|2, -2\rangle$), which we balanced to maintain roughly equal numbers of both isotopes. After 10 s of evaporative cooling, Bose-Einstein condensation of ${}^7\text{Li}$ occurs together with a ${}^6\text{Li}$ degenerate Fermi gas (fig.3). Surprisingly, a single 25 s ramp performed only on ${}^6\text{Li}$ achieved the same results. In this case the equal number condition was fulfilled because of the reduced lifetime of the ${}^7\text{Li}$ cloud that we attribute to dipolar collisional loss [17].

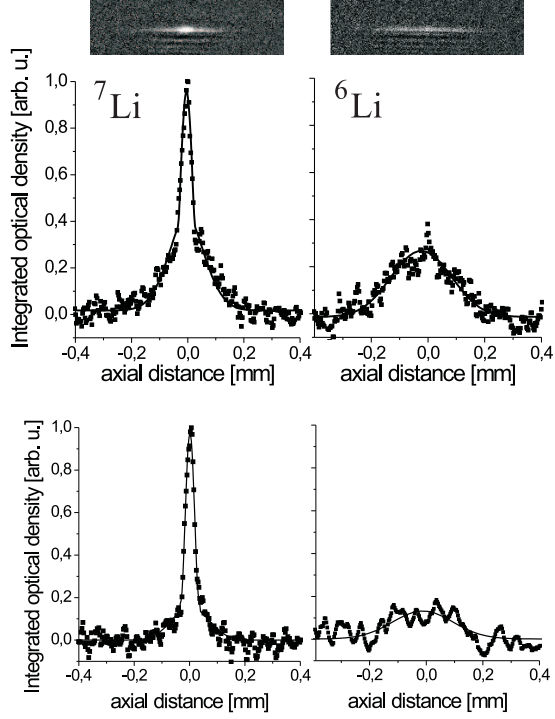


FIG. 3. Mixture of Bose and Fermi gases. Top: In situ spatial distributions after sympathetic cooling with $N_B = 3.5 \cdot 10^4$ and $N_F = 2.5 \cdot 10^4$. The Bose condensed peak ($8.5 \cdot 10^3$ atoms) is surrounded by the thermal cloud which allows the determination of the common temperature. $T = 1.6 \mu\text{K} = 0.87 T_C = 0.57 T_F$. The Fermi distribution is wider because of the smaller magnetic moment and Fermi pressure. Bottom: profiles with a *quasi-pure* condensate, with $N_B = 1.5 \cdot 10^4$, $N_F = 4 \cdot 10^3$. The barely detectable thermal cloud indicates a temperature of $\simeq 0.28 \mu\text{K} \simeq 0.2(1) T_C = 0.2(1) T_F$.

The duration of the RF evaporation ramp was matched to this loss rate. In the following we concentrate on this second, and simpler, evaporation scheme, sympathetic cooling of ^7Li by evaporative cooling of ^6Li .

In fig.3 in-situ absorption images of bosons and fermions at the end of the evaporation are shown. The bosonic distribution shows the typical double structure: a strong and narrow peak forms the condensate at the center, surrounded by a much broader distribution, the thermal cloud. As the Fermi distribution is very insensitive to temperature, this thermal cloud is a very useful tool for the determination of the common temperature. Note that, as cooling was only performed on ^6Li atoms, the temperature measured on ^7Li cannot be lower than the temperature of the fermions. Measuring N_B , N_F , the condensate fraction N_0/N_B , and $\bar{\omega}$, we determine the quantum degeneracy of the Bose and Fermi gases. In fig.3(top), the temperature is just below T_C , $T = 1.6 \mu\text{K} = 0.87 T_C = 0.57 T_F$. In fig.3(bottom) on the contrary, the condensate is quasi-pure; $N_0/N_B = 0.77$; the thermal fraction is near our detectivity limit, indicating a temperature of $\simeq 0.28 \mu\text{K} \leq 0.2 T_C = 0.2 T_F$ with $N = 8.2 \cdot 10^3$

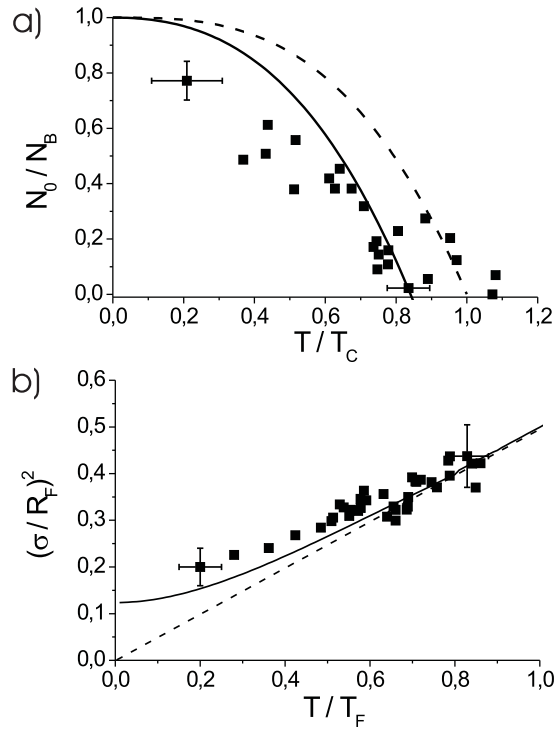


FIG. 4. Temperature dependence of mixtures of quantum gases: a) normalized BEC fraction as a function of T/T_C . Dashed line: theory in the thermodynamic limit. Solid line: theory including finite size and trap anisotropy [2]; b) fermion cloud size: variance of gaussian fit divided by the square of Fermi radius $R_F^2 = 2k_B T_F / M \omega_{ax}^2$ as a function of T/T_F . Solid line: theory. Dashed line: Boltzmann gas.

bosons and 410^3 fermions. Clearly a more sensitive thermal probe is required now to investigate the temperature domain $T < 0.2 T_F$. An elegant method uses the measurement of thermalization rates with impurity atoms including Pauli blocking [20,21]. The condensate fraction N_0/N_B as a function of T/T_C is shown in fig.4 (a), while the size of the fermi gas as a function of T/T_F is shown in fig.4 (b). With the strong anisotropy ($\omega_{rad}/\omega_{ax} = 59$) of our trap, the theory including anisotropy and finite number effects differs significantly from the thermodynamic limit [2], in agreement with our measurements even though there is a 20% systematic uncertainty on our determination of T_C and T_F .

Because of the small scattering length, this ^7Li condensate has interesting properties. The time of flight images, performed after expansion times of 0-10 ms with $N_0 = 10^4$ condensed atoms, reveal that the condensate is a one-dimensional (1D) condensate. In contrast to typical condensates in the Thomas-Fermi (TF) regime, where the release of interaction energy leads to a fast increase in radial size, our measurements agree to better than 5% with the time development of the radial ground state wave function in the harmonic magnetic trap (fig.5). This behavior is

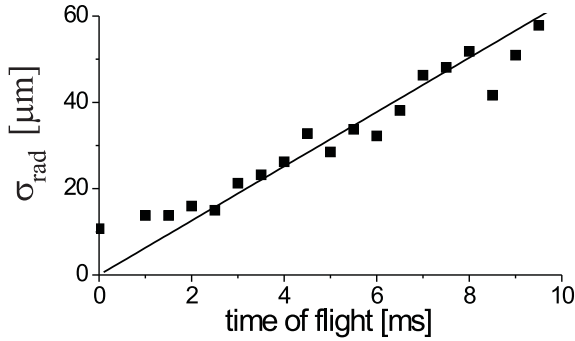


FIG. 5. Signature of 1D condensate. Radial size of expanding condensates with 10^4 atoms as a function of time of flight. The straight line is the expected behavior for the expansion of the ground state radial harmonic oscillator.

expected when the chemical potential μ satisfies the condition $\mu < \hbar\omega_{\text{rad}}$. Searching for the ground state energy of the many-body system with a Gaussian ansatz radially and TF shape axially [13], we find that the mean-field interaction increases the size of the Gaussian by $\approx 3\%$. The calculated TF radius is $28 \mu\text{m}$ or 7 times the axial harmonic oscillator size and is in good agreement with the measured radius, $30 \mu\text{m}$ in fig. 3. Thus with $\mu = 0.45 \hbar\omega_{\text{rad}}$, the gas is described as an ideal gas radially but is in the TF regime axially. This 1D situation was also realized recently in sodium condensates [14]. As $\mu < \hbar\omega_{\text{rad}}$ implies that the linear density of a 1D condensate is limited to $\simeq 1/a$, the 1D regime is much easier to reach with ^7Li (small a) than with Na or ^{87}Rb which have much larger scattering lengths.

What are the limits of this BEC-Fermi gas cooling scheme? First, the $1/e$ condensate lifetime of about 3 s in this steep trap will limit the available BEC-Fermi gas interaction time. Second, the boson-fermion mean field interaction can induce a spatial phase separation [8] that prevents thermal contact between ^7Li and ^6Li . Using the method of [8] developed for $T = 0$, we expect, for the parameters of fig.3 (top), that the density of fermions is only very slightly modified by the presence of the condensate in accordance with our observations. Third, because of the superfluidity of the condensate, impurity atoms (such as ^6Li), which move through the BEC slower than the sound velocity v_c , are no longer scattered [9,16]. When the Fermi velocity v_F becomes smaller than v_c , cooling occurs only through collisions with the bosonic thermal cloud, thus slowing down drastically. With 10^4 condensed atoms, the velocity is $\simeq 0.9 \text{ cm/s}$, corresponding to a limiting temperature of about 100 nK, a factor 3 lower than our currently measured temperature.

In summary, we have produced a new mixture of Bose and Fermi quantum gases. Future work will explore the degeneracy limits of this mixture with the sensitive temperature probe mentioned above [20]. Phase fluctuations of the 1D ^7Li condensate should

also be detectable via density fluctuations in time of flight images, as recently reported in [23]. The transfer of the BEC into $|F = 2, m = 2\rangle$ with negative a should allow the production of bright solitons and of large unstable condensates where interesting and still unexplained dynamics has been recently observed [11,24]. Finally, the large effective attractive interaction between ^6Li $|F = 1/2, m_F = +1/2\rangle$ and $|F = 1/2, m_F = -1/2\rangle$ makes this atom an attractive candidate for searching for BCS pairing if the temperature can be made sufficiently low [6].

We are grateful to Y. Castin, J. Dalibard, C. Cohen-Tannoudji, and G. Shlyapnikov for useful discussions. F. S., and K. C. were supported by a fellowship from the DAAD and by MENRT. This work was supported by CNRS and Collège de France. Laboratoire Kastler Brossel is *Unité de recherche de l'École Normale Supérieure et de l'Université Pierre et Marie Curie, associée au CNRS*.

-
- [1] Proc. of the Int. School of Phys. "Enrico Fermi", M. Inguscio, S. Stringari and C. Wieman eds, (IOS Press, Amsterdam 1999).
 - [2] F. Dalfovo *et al.*, Rev. Mod. Phys. **71**, 463 (1999).
 - [3] B. DeMarco and D. Jin, Science **285**, 1703 (1999).
 - [4] F. Schreck *et al.*, Phys. Rev. A, **64**, 011402R (2001).
 - [5] A. Truscott *et al.*, Science **291**, 2570 (2001).
 - [6] H. Stoof *et al.*, Phys. Rev. Lett., **76**, 10 (1996).
 - [7] C. Ebner and D. Edwards, Phys. Rep., **2C**, 77 (1970).
 - [8] K. Mølmer, Phys. Rev. Lett., **80**, 1804 (1998).
 - [9] E. Timmermans and R. Côté, Phys. Rev. Lett., **80**, 3419 (1998).
 - [10] C. Bradley, C. Sackett, and R. Hulet, Phys. Rev. Lett. **78**, 985 (1997).
 - [11] J. Gerton *et al.*, Nature **408**, 692 (2000)
 - [12] R. Hulet, private communication
 - [13] D. Petrov, G. Shlyapnikov and J. Walraven, Phys. Rev. Lett., **85**, 3745 (2000).
 - [14] A. Görlitz *et al.*, cond-mat/0104549 (2001).
 - [15] M.-O. Mewes *et al.*, Phys. Rev. A **61**, 011403R, (2000).
 - [16] A. Chikkatur *et al.*, Phys. Rev. Lett. **85**, 483, (2000).
 - [17] F. Van Abeelen, B. Verhaar, and A. Moerdijk, Phys. Rev. A **55**, 4377 (1997).
 - [18] D. Butts and D. Rokhsar, Phys. Rev. A **55**, 4346 (1997).
 - [19] B. DeMarco and D. Jin, Phys. Rev. A **58**, 4267 (1998).
 - [20] G. Ferrari, Phys. Rev. A. **59**, R4125 (1999).
 - [21] B. DeMarco, S. Papp and D. Jin, Phys. Rev. Lett., **86**, 5409, (2001).
 - [22] T. Busch *et al.*, Europhys. Lett., **44**, 755 (1998).
 - [23] S. Dettmer *et al.*, cond-mat/0105525 (2001)
 - [24] J. Roberts *et al.*, Phys. Rev. Lett. **86**, 4211 (2001)